

Laser emission in proton-implanted Nd:YAG channel waveguides

E. Flores-Romero^{1*}, G. V. Vázquez², H. Márquez¹ and R. Rangel-Rojo¹, J. Rickards³ and R. Trejo-Luna³

¹ Departamento de Óptica, CICESE, Km 107 Carr. Tijuana-Ensenada, 22860 Ensenada, B.C., México

² Centro de Investigaciones en Óptica, Loma del Bosque 115, Lomas del Campestre, 37150 León, Guanajuato, México

³ Instituto de Física, Universidad Nacional Autónoma de México, Apartado Postal 20364, México D.F. 01000, México

*Corresponding author: floresr@cicese.mx

Abstract: The performance of lasers based on channel waveguides produced by proton implantation in Nd:YAG crystals through an electroformed mask is reported. The fabrication method used can produce several waveguide lasers in the crystal by a single implantation process with very good optical performance. The analysis and comparison of the main laser emission features, as well as the propagation losses of these waveguides, by using different output couplers in the laser cavity is also presented.

©2007 Optical Society of America

OCIS codes: (230.7380) Waveguides, channelled; (140.3070) Infrared and far-infrared lasers; (140.3380) Laser materials; (140.3530) Lasers, neodymium; (140.3580) Lasers, solid-state.

References and links

1. P.D. Townsend, P.J. Chandler and L. Zhang, *Optical effects of ion implantation* (Cambridge University Press, 1994).
2. E. Flores-Romero, G. V. Vázquez, H. Márquez, R. Rangel-Rojo, J. Rickards and R. Trejo-Luna, "Optical channel waveguides by proton and carbon implantation in Nd:YAG crystals," *Opt. Express* **15**, 8513-8520 (2007).
3. M. Szachowicz, P. Moretti, M.F. Joubert, M. Couchaud and B. Ferrand, "Fabrication of H⁺ implanted channel waveguides in Y₃Al₅O₁₂:Nd,Tm single crystal buried epitaxial layers for infrared to blue upconversion laser systems," *Appl. Phys. Lett.* **90**, 0131113 (2007).
4. L. Zhang, P.J. Chandler, P.D. Townsend, S.J. Field, D.C. Hanna, D.P. Shepherd and A.C. Tropper, "Characterization of ion implanted waveguides in Nd:YAG," *J. Appl. Phys.* **69**, 3440-3446 (1991).
5. G.V. Vázquez, J. Rickards, H. Márquez, G. Lifante, E. Cantelar and M. Domenech, "Optical waveguides in Nd:YAG by proton implantation," *Opt. Commun.* **218**, 141-146 (2003).
6. G.V. Vázquez, J. Rickards, G. Lifante, M. Domenech and E. Cantelar, "Low dose carbon implanted waveguides in Nd:YAG," *Opt. Express* **11**, 1291-1296 (2003).
7. P.J. Chandler, S.J. Field, D.C. Hanna, D.P. Shepherd, P.D. Townsend, A.C. Tropper and L. Zhang, "Ion-implanted Nd:YAG planar waveguide laser," *Electron. Lett.* **25**, 985-986 (1989).
8. S.J. Field, D.C. Hanna, D.P. Shepherd, A.C. Tropper, P.J. Chandler, P.D. Townsend and L. Zhang, "Ion-implanted Nd:YAG waveguide lasers," *IEEE J. Quantum Electron.* **27**, 428-433 (1991).
9. M. Domenech, G.V. Vázquez, E. Cantelar and G. Lifante, "CW laser action at $\lambda = 1064.3$ nm in proton and carbon implanted Nd:YAG waveguides," *Appl. Phys. Lett.* **83**, 4110-4112 (2003).
10. E. Flores-Romero, G. V. Vázquez, H. Márquez, R. Rangel-Rojo, J. Rickards and R. Trejo-Luna, "Planar waveguide lasers by proton implantation in Nd:YAG crystals," *Opt. Express* **12**, 2264-2269 (2004).
11. P. Moretti, M.F. Joubert, S. Tascu, B. Jacquier, M. Kaczkan, M. Malinowskii and J. Samecki, "Luminescence of Nd³⁺ in proton or helium-implanted channel waveguides in Nd:YAG crystals," *Opt. Mater.* **24**, 315-319 (2003).
12. S.J. Field, D.C. Hanna, A.C. Large, D.P. Shepherd, A.C. Tropper, P.J. Chandler, P.D. Townsend and L. Zhang, "Low threshold ion-implanted Nd:YAG channel waveguide laser," *Electron. Lett.* **27**, 2375-2376 (1991).
13. J.F. Bourhis, "Fibre to waveguide connection," in *Glass Integrated Optics and Optical Fiber Devices*, S.I. Najafi, ed., SPIE Critical Reviews of Optical Science and Technology **CR53**, 335-366 (1994).
14. R. Paschotta, "Lasers," *Encyclopedia of Laser Physics and Technology* (RP Photonics Consulting GmbH, 2007). <http://www.rp-photonics.com/lasers.html>

1. Introduction

There is a growing need in the integrated optics field to miniaturize laser devices to make these compatible with semiconductor lasers and fiber optics technology. One avenue towards these miniature lasers relies on optical waveguides with the capability of supporting laser oscillation, that is, *optical waveguide lasers*. An optical waveguide laser presents some advantages over a laser based on a bulk configuration, e.g. high power densities, high optical gain per unit pump power, and compatibility with semiconductor lasers and fiber optics technology. These properties allow waveguide lasers to exhibit higher slope efficiencies and lower threshold pump powers than those obtained for a bulk configuration.

The optical waveguide fabrication method and the laser material used are crucial issues to obtain good quality waveguides. On the one hand, ion implantation is one of several techniques that have been employed to fabricate optical waveguides [1]; the effectiveness of ion implantation derives from the reproducibility and controllability of the results [2,3]. On the other hand, for Nd:YAG, which is one of the most important solid state laser materials, optical waveguide formation by ion implantation has been successfully demonstrated [1].

Planar waveguides in Nd:YAG have been obtained by helium, proton and carbon implantation [4-6]. Laser oscillation at 1064 nm in these planar structures has also been reported [7-10]. However, in order to take advantage of the waveguide structure, a more useful configuration is achieved with channel instead of planar waveguides. In this regard, channel waveguides in Nd:YAG have been obtained by implantation of helium ions [8,11], protons [2,3,11] and carbon ions [2]; nevertheless laser oscillation in such channel structures has only been reported for those obtained by helium implantation [12]. This suggests that laser performance in waveguides obtained with other ion species should be explored. We were encouraged to use protons because it has been shown that the use of these ions to fabricate waveguides has the advantage of producing fewer deleterious effects on the optical properties of the Nd:YAG crystal, even when high doses are employed [5].

One method for producing channel waveguides by ion implantation requires the use of a mask that stops the ions completely, and allows implantation only in the region to become a channel [1]. Several attempts of implantation masks have been made, one of them a photolithographically patterned gold film with a thickness of $\sim 3 \mu\text{m}$, with which several waveguides of different widths were obtained; unfortunately, the film did not fully stop the ions as required [8,12]. Another implantation mask is a moving slit setup, which effectively stops the ions, but it only allows the production of one waveguide at a time on the same crystal [11]. In this context, recently we have successfully demonstrated an alternative masking technique (an electroformed mask) to form optical channel waveguides. The mask used is thick enough to fully stop the ions, and permits the formation of several sets of optical channels with different widths under the same implantation conditions, e.g. by a single implantation process [2]; this offers a great potential for large-scale production.

This work reports the study of laser performance at 1064 nm in channel waveguides obtained by proton implantation in Nd:YAG crystals through an electroformed mask. A comparison of the main laser features, i.e. slope efficiency and threshold pump power, and the propagation losses obtained by using several output couplers in the laser cavity is presented.

2. Experimental details

Several sets of channel waveguides with different widths were obtained by a room-temperature proton implantation on a commercial Nd:YAG (1.0% at.) crystal through an electroformed mask [2]. The implantation was performed using a 9SDH-2 Pelletron Accelerator. The protons, with energies around 1.0 MeV, impinged onto the crystal at an angle of 61° with respect to the surface normal of the crystal and the total dose was 2.0×10^{16} protons/cm²; more details about the fabrication method are described in [2].

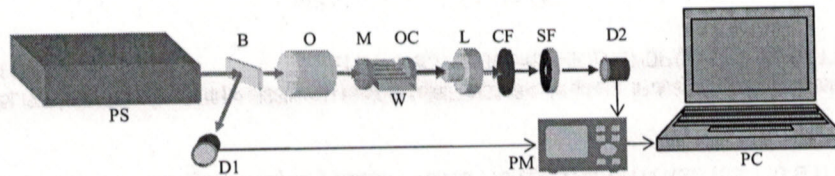


Fig. 1. Experimental setup used to obtain laser oscillation. PS, pumping source; B, beam splitter; O, microscope objective; M, input mirror; W, channel waveguides; OC, output coupler; L, aspheric lens; CF, color filter; SF, spatial filter; D1 and D2, detectors; PM, power meter; PC, personal computer.

The setup used to test the laser properties of the channel waveguides is sketched in Fig. 1. A continuous-wave Ti:Sapphire laser, tuned to a wavelength of 808 nm, was used as pump. A detector received the beam reflected by a beam splitter; this beam was used as a reference to monitor the pump power incident on the laser cavity. The pump beam was end-coupled into the laser cavity via a 10X microscope objective. The laser cavity was formed by dielectric mirrors held onto the polished end-faces of the channel waveguides. To ensure good contact between the waveguide end-face and the mirrors, a thin layer of low-fluorescence microscope immersion oil was used (this oil was not selected to match the refractive index of the substrate). The input mirror was highly reflective ($R > 99\%$) at the laser wavelength, 1064 nm, while its transmission for the pump wavelength was about 75%. Three different output mirrors were used to perform the test, the transmissions at 1064 nm were: 9.0, 10.5 and 21.5%; hereafter these output couplers will be denoted by OC-09, OC-10 and OC-20, respectively. The waveguide output was collected by an aspheric lens which has antireflection coatings in the 1050-1500 nm wavelength range. The collected beam was directed to a second detector. The detectors were connected to a power meter, in turn connected to a personal computer, to measure the input and output power simultaneously. Before the detector D2 a color filter and a spatial filter were used to eliminate the remaining pump light and the fluorescence from the bulk, respectively. In order to optimize the coupling, the microscope objective, the crystal with the waveguides (together with the mirrors) and the aspheric lens were controlled by separate micro-positioning stages.

3. Results and discussion

The optical waveguide laser array obtained in a Nd:YAG crystal contains three sets of ten channels with widths of 10, 15 and 20 μm respectively; all channels are located on the same crystal surface and are 10 mm long, and approximately 4.6 μm deep. Since all the channels were successful at guiding light, each one was tested in order to determine its laser operation for a given output coupler, and its corresponding slope efficiency curve was obtained.

The slope efficiency curve is the plot of the laser output power as a function of the absorbed pump power. In order to calculate the pump power absorbed by the waveguides, it was assumed that all the light launched into each waveguide was fully absorbed (this assumption is justified since the typical absorption coefficient of Nd:YAG, 1.0% at., at 808 nm is about 6 cm^{-1} and thus the percentage of absorbed power for 1.0 cm length is $\sim 99.75\%$). The light launched into one waveguide was estimated taking into account the following: the transmission of the microscope objective used to focus the laser beam, the input mirror transmission at the pump wavelength, and the mode coupling between the guided mode of the waveguide and the mode of the input beam [13]. Therefore, coupling efficiency into one waveguide was 35.6, 29.2 or 26.6%, depending on the waveguide width, 10, 15 or 20 μm , respectively.

Analysis of the slope efficiency curve allows the determination of two very important laser features, the slope efficiency (ϕ) and the threshold pump power (P_{th}). The first is defined as the slope of the curve when it is within the linear regime while the threshold pump power is the smallest pump power for which laser action is observed. In other words, at the threshold pump power the small-signal-gain exactly equals the resonator losses [14]. The threshold was

obtained as the point where the fitted line crosses the absorbed pump power axis. Figure 2(a) shows a typical slope efficiency curve for the 15 μm wide waveguide lasers, where it can be seen that for this case $\phi=0.16=16.0\%$ and $P_{\text{th}}\sim 6.9$ mW. In Fig. 2(b) it is possible to recognize the corresponding emission line at 1064.1 nm with a bandwidth, full width at half maximum (FWHM), of 0.21 nm. It should be noted however that some waveguides exhibited two laser emission lines, at 1061.4 (FWHM ~ 0.10 nm) and 1064.1 nm; an example of this behavior is shown in Fig. 2(c). These two lines correlate very well with the strongest two peaks in the fluorescence spectrum of Nd:YAG (centered at 1061.3 and 1064.1 nm [2]). Therefore, it could be expected that the gain of these two lines exceeds the resonator losses, and hence the laser could oscillate simultaneously in both lines.

We measured for each waveguide and output coupler, the slope efficiency and the threshold pump power. As an example, Fig. 3 shows the values of these features obtained for waveguide lasers of different width when the OC-20 output coupler was used (the figure is presented to show the general behavior from the sets of waveguides and not to compare individual waveguides). As it can be noted, the 15 and 20 μm wide waveguides exhibited similar behavior, while the 10 μm waveguides presented both the lowest *average* slope efficiency and the highest *average* threshold pump power. With the OC-10 and OC-09 output couplers, the 10 and 20 μm wide waveguides presented similar behavior in efficiency, while the highest values in this feature were obtained for the 15 μm waveguides; for the threshold pump power, the 15 and 20 μm waveguides presented similar low values, while the 10 μm waveguides exhibited the highest threshold values.

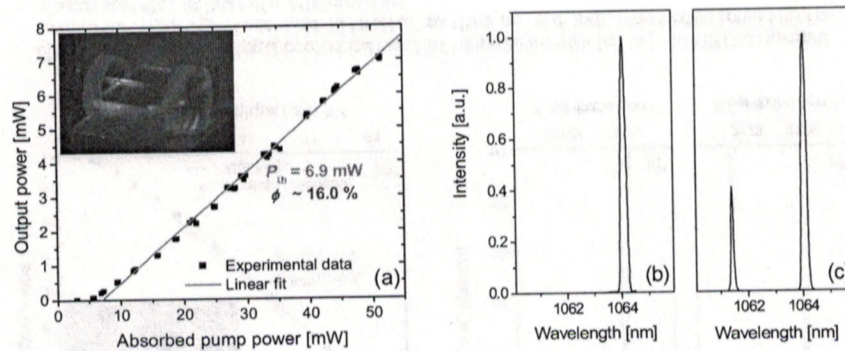


Fig. 2. Typical behavior of channel waveguide lasers of 15 μm in width with the OC-20 output coupler; (a) Slope efficiency curve, the inset shows a photograph of the crystal during the laser performance; (b)-(c) Laser emission spectra.

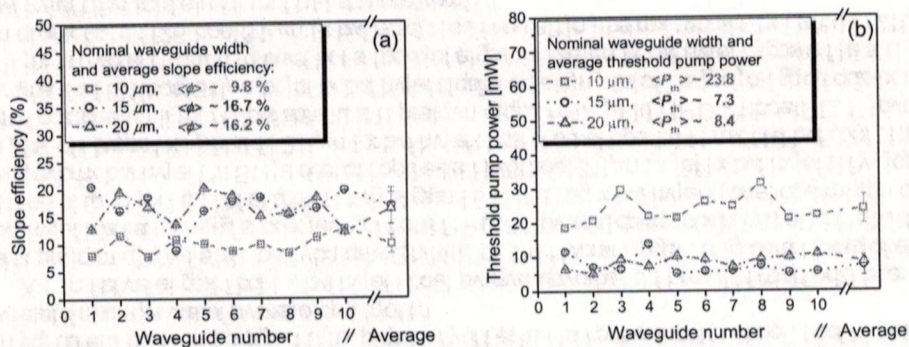


Fig. 3. Characteristics of channel waveguide lasers with the OC-20 output coupler. (a) Slope efficiency, (b) Threshold pump power.

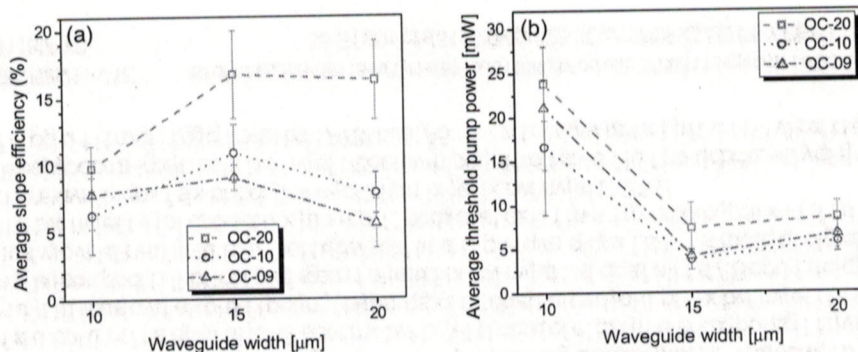


Fig. 4. Characteristics of channel waveguide lasers as function of the waveguide width for several output couplers. (a) Average slope efficiency; (b) Average threshold pump power.

The *average* slope efficiencies and the *average* threshold pump powers obtained from the waveguides for different output couplers are presented in Fig. 4 as function of waveguide width. It can be seen in Fig. 4(a), that the highest *average slope efficiencies* for all groups of waveguides were achieved using the OC-20 output coupler. The lowest average slope efficiencies for the 15 and 20 μm wide waveguides were obtained with the OC-09 output coupler, and for the 10 μm waveguides with the OC-10 output coupler. It can also be seen that for each output coupler used, the best average slope efficiencies were obtained for the 15 μm wide waveguides. The efficiencies obtained here are higher than those reported in planar implanted planar waveguides [7,8], but they are smaller than those reported in helium waveguides obtained under similar conditions [10]. Also they are similar to those obtained in planar waveguides fabricated by a multiple energy implant of protons or by a single energy implant of carbon ions [9]; and they are smaller than those presented in channel waveguides obtained by a multiple energy implant of helium ions [12]. It must be noted however, that all the waveguides reported in these previous works were subjected to an annealing step which is not the case of the channel waveguides reported here, since no post-implant treatment was carried out yet.

Concerning the *average threshold pump power*, Fig. 4(b) makes it clear that for all waveguides the lowest average threshold pump powers were obtained with the OC-10 output coupler, while the highest were obtained with the OC-20 output coupler. Figure 4(b) also makes it clear that for each output coupler used, the 15 μm wide waveguides presented the lowest average threshold pump powers ($P_{th} \sim 3.7\text{--}7.3$ mW), the 20 μm wide waveguides presented slightly higher average threshold pump powers ($P_{th} \sim 5.7\text{--}8.4$ mW), and the 10 μm waveguides showed the highest average threshold pump powers ($P_{th} \sim 16.6\text{--}23.8$ mW). It should be noted that the maximum average threshold pump power for the 15 and 20 μm wide waveguides are even lower than the minimum for the 10 μm waveguides. Clearly, waveguides with different widths lead to different lasing behaviors. Comparing these results with those obtained in previous works, it is found that there is a reduction in the threshold pump power by a factor of ten with respect to planar waveguides obtained under similar conditions [10]. The values are smaller than those reported in planar waveguides obtained by a multiple energy implant of protons [10] or by a single energy implant of carbon ions [9]. Finally, they are higher than those reported in channel waveguides obtained by implantation of helium ions [12]; this is attributed to the optimization process carried out in those waveguides while no optimization process has been performed in the waveguides reported here. Another difference with previous results is that the best average threshold pump powers were obtained for 15 μm wide waveguides, in contrast with those obtained by helium implantation where the best threshold pump power was achieved in 20 μm wide waveguides [12].

Additionally, for slab waveguides and bulk optics lasers, the theoretical and experimental values of the slope efficiency are ~62 and ~49%, respectively; while these values for the

threshold pump power are both ~ 30 mW [15]. The experimental efficiencies obtained for ion implanted waveguide lasers range from ~ 2 to 29%; and the threshold pump powers range from ~ 1 to ~ 50 mW [7-10,12]. Waveguides usually exhibit more propagation losses than slab and bulk configurations, thus producing low efficiencies; however the threshold pump power is indeed substantially reduced due to the high sustained pump and lasing power densities attainable along the entire cavity because of waveguide structure [1].

With the OC-20 output coupler it is possible to achieve the best average slope efficiency but a greater pump power is also necessary to reach laser oscillation because of the slightly higher threshold power. Note also that, with the OC-10 output coupler it is possible to reduce the threshold pump power but then the slope efficiency is unfortunately also reduced. This behavior is consistent with waveguide laser theory, as can be seen from the following equations that relate the slope efficiency and the threshold pump power with different parameters of the laser cavity and with the waveguide propagation losses [9]:

$$\phi = \eta \frac{1-R_2}{\delta} \frac{\lambda_p}{\lambda_s}, \quad (1)$$

$$P_{th} = \frac{hc}{\lambda_p} \frac{1}{\eta \sigma_e \tau} \frac{\delta}{2} A_{eff}, \quad (2)$$

where η is the fraction of absorbed photons that contribute to the population of level ${}^4F_{3/2}$ ($\eta=1$), $\delta=2\alpha l - \ln(R_1 R_2)$ represents the total cavity losses (α being the propagation loss coefficient at the lasing wavelength), l is the cavity length, R_1 and R_2 are the reflectivities of the input and output mirrors, λ_p and λ_s are the pumping and signal wavelengths, h is the Planck's constant, c is the speed of light in vacuum, $\sigma_e = 3.1 \times 10^{-19}$ cm² is the stimulated emission cross section, $\tau = 240$ μ s is the fluorescence lifetime, and A_{eff} is the effective pump area. From Eq. (1) and Eq. (2), when the reflectivity of the output coupler (R_2) is increased, both the slope efficiency and the threshold pump power are diminished, which is consistent with the behavior observed.

Equation (1) could also be used to calculate the waveguide propagation loss coefficient, if we use the experimental measurements of the waveguide slope efficiency. This calculation was performed for each waveguide and for each output coupler used. The values encountered are: for the 10 μ m wide waveguides, $\alpha=2.7 \pm 1.1$ dB/cm; for waveguides with a 15 μ m width, $\alpha=1.5 \pm 0.5$ dB/cm; and for the 20 μ m wide waveguides, $\alpha=2.1 \pm 0.8$ dB/cm. Clearly, waveguides with different widths present different propagation losses and the waveguides with lowest average propagation losses are the 15 μ m wide.

A major application for a Nd:YAG laser is to obtain green light by frequency doubling, a waveguide laser for this purpose could be generated by means of ion implantation on a composite laser crystal, e.g. a Nd:YAG/KTP monolithic composite crystal fabricated by diffusion bonding for intracavity frequency doubling. Work oriented to the development of these high performance and very compact solid state lasers is now in progress.

4. Conclusion

The laser performance of several channel waveguides obtained by proton implantation in Nd:YAG crystals through an electroformed mask is reported. This alternative masking technique was able to produce several very good optical waveguide lasers with different widths in the same crystal by a single implantation process; the technique then should be compatible with large-scale production.

Three sets of ten channel waveguides with widths of 10, 15 and 20 μ m respectively, were analyzed; the main laser characteristics, i.e. slope efficiency and threshold pump power, in these waveguides for different output couplers were compared. The slope efficiency ranges achieved were 6.3-9.8, 9.0-16.7 and 5.5-16.2% while the threshold pump power ranges were 16.6-23.8, 3.7-7.3 and 5.7-8.4 mW, for waveguides of 10, 15 and 20 μ m in width respectively. These results show that the 15 μ m waveguides present both, the highest efficiency and the

lowest threshold power, although with different output couplers, thus a compromise between these features must be adopted in order to optimize the laser output power as required by the application.

The slope efficiency values were used to calculate the propagation loss coefficient of the waveguides. In general, the values obtained are between 1.0-3.8 dB/cm, the minimum and the maximum corresponding to 15 and 10 μm wide waveguides, respectively. Better efficiencies and lower power thresholds for all waveguides can be achieved by diminishing the waveguide propagation losses and with mirrors fabricated directly over the input and output waveguide end-faces. Efforts will be focused in these directions to improve laser emission features.

Acknowledgments

The authors acknowledge the financial support from CONACyT, Mexico, (doctoral degree scholarship 158414 and projects J42695-F, G0010-E and F036-E9109). We are also thankful to K. López and F. Jaimes for supervising implants.